https://www.scirp.org/journal/ns Natural Science, 2023, Vol. 15, (No. 4), pp: 179-189

Potential Power of the Pyramidal Structure VIII: Exploration of Periodic Diurnal Oscillation of Pyramid Power and Bio-Entanglement

Osamu Takagi[1], Masamichi Sakamoto[2], Kimiko Kawano[1], Mikio Yamamoto[1]

[1]International Research Institute (IRI), Chiba, Japan; [2]Aquavision Academy, Chiba, Japan

Correspondence to: Osamu Takagi, takagi@a-iri.org

Keywords: Pyramid, Potential Power, Bio-Entanglement, Diurnal Oscillation, Biosensor, *Cucumis sativus*, Gas, Psi Index

Received: March 7, 2023 **Accepted:** April 25, 2023 **Published:** April 28, 2023

ABSTRACT

To date, numerous books have been published on so-called "pyramid power" but there have been few academic papers on this subject other than our own. Since 2007, to demonstrate the pyramid power, we have undertaken strictly scientific experiments using a pyramidal structure (PS) that we have carefully constructed. In previous reports, we used the edible cucumber, *Cucumis sativus* as an effective and practical biosensor. Through measurement and analysis of volatile components (gas concentrations) emitted from the biosensor, we were able to demonstrate the existence of the pyramid power and revealed some of its characteristics. In a paper published in 2022, we showed that gas concentration release from this biosensor displayed a circadian rhythm and that this rhythm changed with the season. Based on the result that the biosensor had a periodic diurnal oscillation called a circadian rhythm, we questioned whether or not pyramid power and Bio-Entanglement also had periodic diurnal oscillations. In this paper, we investigated that possibility. Our results have shown that pyramid power and Bio-Entanglement do not exhibit significant periodic diurnal oscillations. Thus we have revealed for the first time that the field associated with pyramid power is a type of static field that always exerts a constant influence. We expect that our research results will be widely accepted in the future and will become the foundation for a new research field in science, with a wide range of applications.

1. INTRODUCTION

Since the late 1930s, there has been increasing interest in the so-called "pyramid power", the unexplained effects of a pyramid. Numerous books have been published on pyramid power to this day [1-18].

However, there have been few scientific experiments conducted to demonstrate or characterize pyramid power and obtain statistically significant data, apart from our research [19].

Since 2007, we have been conducting rigorous scientific experiments to explore the pyramid power phenomenon using pyramidal structure (PS). We use natural biosensors made from slices of commercially available edible cucumbers, *Cucumis sativus* to detect the phenomenon by measuring and analyzing the release of volatile compounds (gas concentration) from the biosensor to demonstrate the existence of the pyramid power and reveal its characteristics. The pyramid power is difficult to detect by regular electrical measuring instruments, and we are conducting pyramid power detection experiments using the biosensors. Our research has resulted in 11 original papers confirming and measuring pyramid power [20-30], 3 original papers on the properties of the cucumber biosensor [31-33], 3 comprehensive reports [34-36], and 1 book chapter [37].

During the analysis of pyramid power using a series of biosensors, we discovered a strange relationship between the sensors. The phenomenon we observed is similar to that of quantum entanglement, so we named it "Bio-Entanglement" [27-29]. Our conclusion was that the psi index Ψ, which had been considered an indicator of the amount of the pyramid power before the discovery of the Bio-Entanglement, turned out to be a combination of the original pyramid power, psi prime index Ψ′ and the Bio-Entanglement, psi double prime index Ψ″ [29].

In our prior 2022 publication [33], we clarified that the gas concentration released from natural biosensors made from a fresh and viable cucumber fruit (a living organism) exhibited a circadian rhythm and that this rhythm changed with the seasons. That is, we revealed that the period of the circadian rhythm was 8 hours in winter, 6 hours in spring, 24 hours in summer, and a mixed period of 12 and 24 hours in autumn. This circadian rhythm is a characteristic of the live cucumber fruit and shows the same rhythm regardless of whether it was influenced by the pyramid power or not.

The purpose of this paper is to examine the question of whether the pyramid power and the Bio-Entanglement also exhibit periodic diurnal oscillation, given the result that the biosensor, a living organism, exhibits a periodic diurnal oscillation called circadian rhythm.

2. EXPERIMENTS

2.1. Pyramidal Structure (PS)

We created the PS shown in **Figure 1(a)**. The PS was a square pyramid with a height of 107 cm, a ridgeline length of 170 cm and a base length of 188 cm. The tilt angle between the bottom and the side of the PS was 49.1˚. The base of the PS was raised to a height of 73 cm from the floor. The frame of the PS was made of four aluminum pipes, each 2 cm in diameter. On the four sides of the PS there was a Sierpinski triangle pattern consisting of aluminum plates. At the PS apex, a Faraday cage for electrostatic shielding of the biosensors was placed. A calibration control point was also set up 8 m away from the PS.

2.2. Preparation, Installation, Storage, and Gas Concentration Measurement of Biosensors

As shown in **Figure 1(b)**, eight uniform biosensors were prepared from four cucumbers. To create uniform biosensors, each Petri dish contained one slice from each of the four cucumbers. Where G_{E1}-G_{E4}, G_{C1}-G_{C4} represent the eight Petri dishes as well as the gas concentration (ppm) emitted from the biosensor in each Petri dish. Eight uniform biosensors were required for each set of experiments to analyze the presence or absence of the pyramid power from the gas concentrations, using the Simultaneous Calibration Technique (SCAT) developed by the International Research Institute (IRI) [38]. SCAT is a sensing method that uses the biosensors, which are considered to be environmentally responsive, high-sensitivity sensors, to clarify spatial characteristics. In the experiment, the biosensors G_{E1} and G_{E2} were placed on top of each other at the PS apex as shown in **Figure 1(b)**, **Figure 1(c)**, while the other biosensors G_{C1}, G_{C2}, G_{E3}, G_{E4}, G_{C3} and G_{C4} were placed at the calibration control point 8 m away from the PS apex with two biosensors on top of each other (**Figure 1(b)**). The biosensors G_{E3}, G_{E4}, G_{C3}, and G_{C4} in pairs 3 and 4 were in the

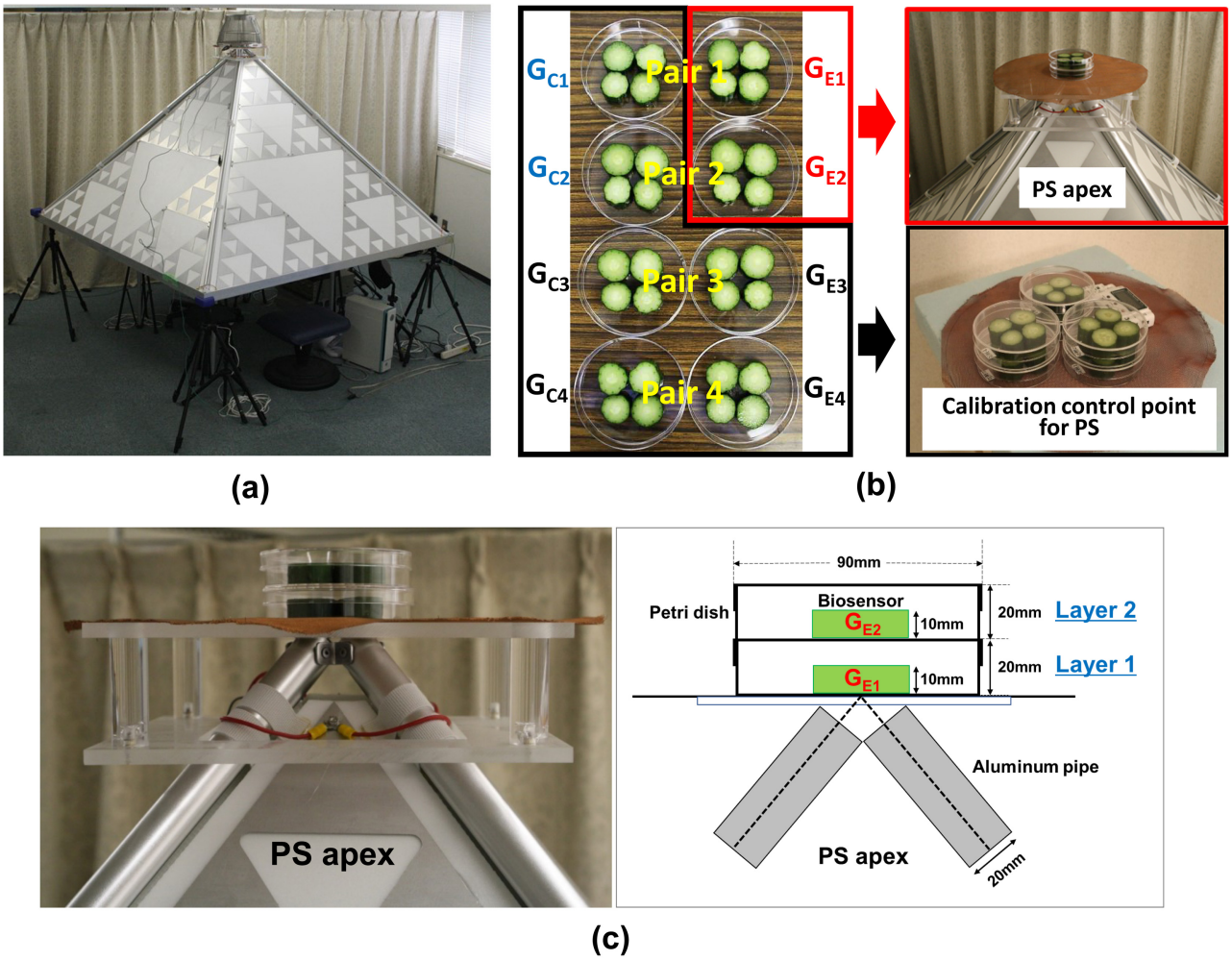

Figure 1. Installation status of the pyramidal structure and the biosensors used in the experiment. (a) The pyramidal structure (PS). (b) Left: The biosensors prepared according to SCAT. (b) Right: The biosensors placed at the PS apex and calibration control point. (c) Left: Photograph of the biosensors at the PS apex. (c) Right: Schematic diagram.

same environment from preparation to placement at the calibration control point, so they were considered to be control samples with the same biological reaction for gas generation.

After leaving the biosensors at the PS apex and calibration control point for 30 minutes, the lids of the Petri dishes were removed and the dishes were placed in a sealed polypropylene container with a volume of 2.2 liters, which was kept in a temperature-controlled (22˚C - 24˚C) room away from direct sunlight for 24 - 48 hours. During storage, gas concentrations reached a maximum after approximately 12 hours and then remained at equilibrium [39]. Gas concentration measurements were taken by suctioning 300 ml of gas from the sealed container using a gas detector (GV-100, Gastec, Japan) and gas detection tubes (141 L, Gastec).

3. DATA ANALYSIS

3.1. The Psi Index Ψ and Psi Prime Index Ψ', a Measure of the Magnitude of the Pyramid Power, and Psi Double Prime Index Ψ", a Measure of the Magnitude of the Bio-Entanglement

The definition formulas for the psi index Ψ, psi prime index Ψ', and psi double prime index Ψ", as

well as a schematic diagram with eight biosensors, G_{E1}-G_{E4} and G_{C1}-G_{C4}, are shown in Figure 2. Equations (1)-(5) in Figure 2 were used as an indicator of the magnitude of the pyramid power until the discovery of the Bio-Entanglement phenomenon. To detect the pyramid power, we adopted SCAT, which can correct for various factors that affect gas concentration released from cucumber slices and calibrated individual differences in cucumber specimens and environmental variations between experiments. Additionally, we calibrated the effect of differences in height when placing the biosensors in two layers. The pyramid power for the biosensors obtained through calibration is expressed as the calibrated psi index $\Psi_{1(E\text{-}CAL)Layer1}$ and $\Psi_{2(E\text{-}CAL)Layer2}$ in Equation (4) in Figure 2. However, our previous reports [27-29] suggested the possibility of the Bio-Entanglement among biosensors. It was found that Bio-Entanglement was noticeable when the biosensors G_{E1} and G_{E2} were affected by the pyramid power, and the gas concentration of G_{C1} and G_{C2}, which form a pair with G_{E1} and G_{E2}, were also affected. Therefore, we understood that both the pyramid power and the Bio-Entanglement were mixed in the calibrated psi index $\Psi_{1(E\text{-}CAL)Layer1}$ and $\Psi_{2(E\text{-}CAL)Layer2}$ in Equation (4) in Figure 2. In Figure 2, the biosensors G_{E1} and G_{E2}, which were affected by the pyramid power, are shown in red, and G_{C1} and G_{C2}, which were affected by the Bio-Entanglement, are shown in blue.

Separation of the calibrated psi index Ψ, which is an indicator of the magnitude of the pyramid power,

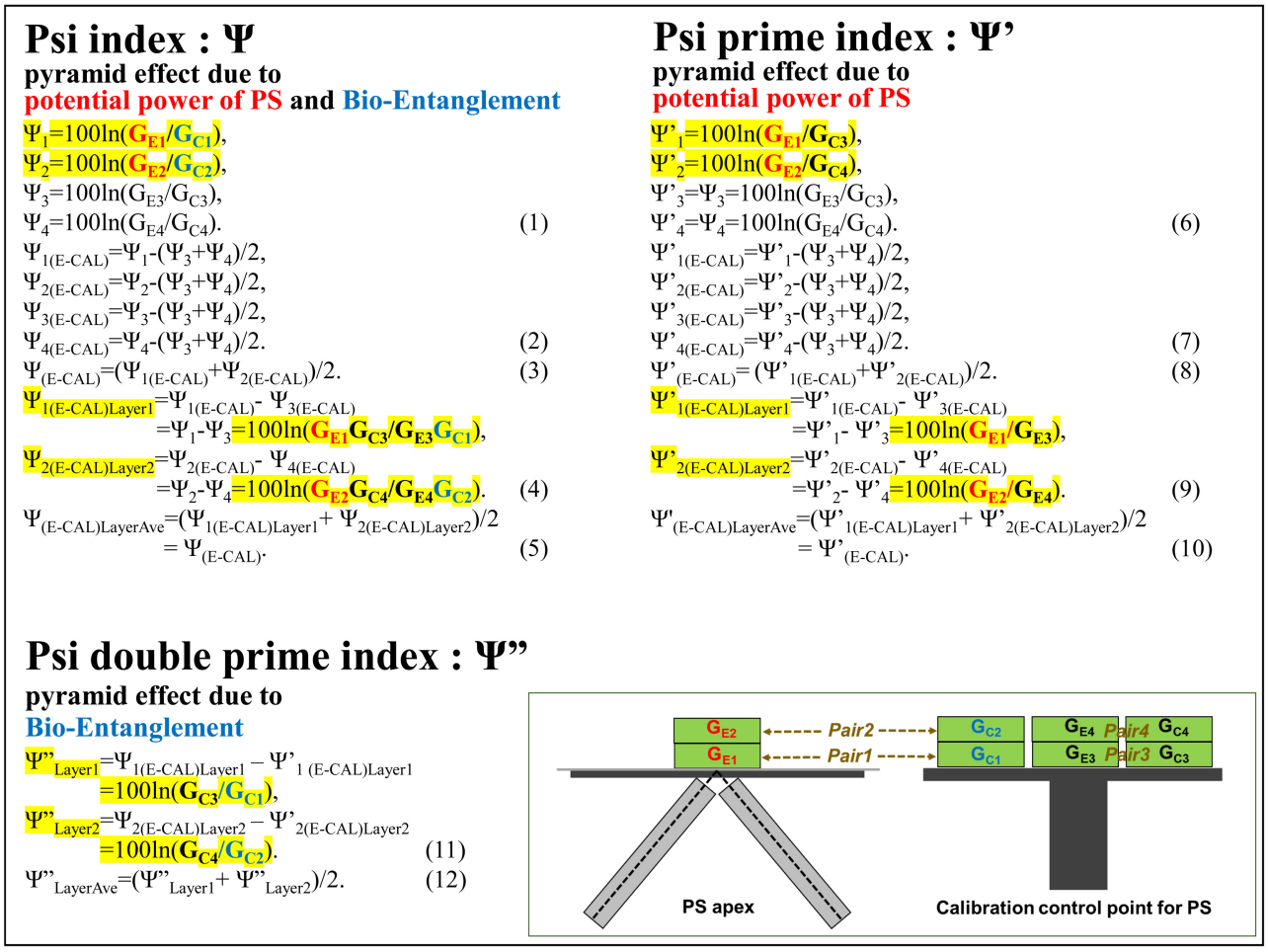

Figure 2. Definition of psi index Ψ, psi prime index Ψ', psi double prime index Ψ" and the schematic diagram of biosensors of the PS apex and calibration control point. G_{E1} and G_{E2} affected by the potential power of the PS are shown in red, and G_{C1} and G_{C2} affected by the Bio-Entanglement are shown in blue. Refer to Section 3-1 for further details on the equations.

into pyramid power and the Bio-Entanglement components, is now respectively defined as the psi prime index Ψ' and psi double prime index Ψ". Therefore, the calibrated psi index Ψ in Equation (4) in **Figure 2** became the psi prime index $\Psi'_{1(\text{E-CAL})\text{Layer1}}$, $\Psi'_{2(\text{E-CAL})\text{Layer2}}$ in Equation (9) in **Figure 2** for the pyramid power, and the Bio-Entanglement became the psi double prime index Ψ''_{Layer1} and Ψ''_{Layer2} in Equation (11) in **Figure 2**.

3.2. Periodic Approximation Curve

To verify the presence of periodic diurnal oscillations in the data, a periodic approximation curve shown in Equation (1) was used.

$$y = a + b\sin(2\pi xN) + c\cos(2\pi xN) = a + \sqrt{b^2 + c^2}\sin(2\pi xN + \phi),\ \phi = \arcsin\left(\frac{c}{\sqrt{b^2 + c^2}}\right) \quad (1)$$

In Equation (1), y represents the data value, and x represents the time, with values ranging from 0 to 1 corresponding to 0 to 24 hours. This assumption was made based on the data changing in a way that matches its value and phase every 24 hours, which by definition are periodic diurnal oscillations. N represents the number of cycles per 24 hours, with N being an integer from 1 to 24. Equation (1) represents the periodic approximation curve for one cycle per 24 hours, 1 cycle per 24 hours when N = 1, and the periodic approximation curve for 24 cycles per 24 hours, 1 cycle per 1 hour when N = 24. a, b, and c are constants, and π represents pi. In this paper, for each value of N from 1 to 24, the periodic approximation curves for the psi prime index $\Psi'_{1(\text{E-CAL})\text{Layer1}}$, $\Psi'_{2(\text{E-CAL})\text{Layer2}}$ and the psi double prime index Ψ''_{Layer1}, Ψ''_{Layer2} were determined, and the constants a, b, and c were determined. Then, the correlation coefficient between each index and its periodic approximation curve were calculated. If significance is associated with the correlation coefficient, it can be concluded that each index has the same periodicity as its periodic approximation curve.

4. ANALYSIS RESULTS

The data used to analyze whether pyramid power and Bio-Entanglement exhibit periodic diurnal oscillations is the same data used in the seven-paper series "Potential Power of the Pyramidal Structure I-VII" [24-30], as well as in our previous paper [33]. The entire data set (n = 468) was divided by season into winter WTR (n = 84), spring SPR (n = 108), summer SMR (n = 144), and autumn AUT (n = 132) for analysis (**Table 1**).

Table 1. Seasonal classification and period, and the number of data for each season.

Classification	Season	Period		Number of data
WTR	winter	from the winter solstice to the day before the spring equinox	from 12/22 to 3/20	84
SPR	spring	from the spring equinox to the day before the summer solstice	from 3/21 to 6/20	108
SMR	summer	from the summer solstice to the day before the autumn equinox	from 6/21 to 9/22	144
AUT	autumn	from the autumn equinox to the day before the winter solstice	from 9/23 to 12/21	132

Figure 3 shows the correlation coefficients between the psi prime index $\Psi'_{1(E\text{-}CAL)Layer1}$, $\Psi'_{2(E\text{-}CAL)Layer2}$, which represent the pyramid power and its periodic approximation curve, as well as the correlation coefficients between the psi double prime index Ψ''_{Layer1}, Ψ''_{Layer2}, which represent the Bio-Entanglement and its periodic approximation curve. The vertical axis shows the correlation coefficient, and the horizontal axis shows the number of cycles per 24 hours of the periodic approximation curve, N, ranging from 1 to 24 integers. The three dashed lines parallel to the x-axis in the figure represent the significance of the different correlation coefficients depending on the number of data points. The red dashed line represents $p = 10^{-5}$, the green dashed line represents $p = 10^{-4}$ and the blue dashed line represents $p = 10^{-3}$. Figures 3(a)-(d) show the results for WTR, SPR, SMR, and AUT, respectively. From the results in Figure 3, in most cases, the significance of the correlation coefficients did not exceed the threshold, so we concluded that the pyramid power and the Bio-Entanglement have little to no periodic diurnal oscillations.

5. CONSIDERATION

Figure 4 shows the correlation coefficients between the release gas concentrations (G_{E1}, G_{E2}, G_{E3}, G_{E4}, G_{C1}, G_{C2}, G_{C3}, G_{C4}) and their periodic approximations. Similar to Figure 3, the vertical axis represents the correlation coefficient, while the horizontal axis represents the number of periods (N) in the periodic

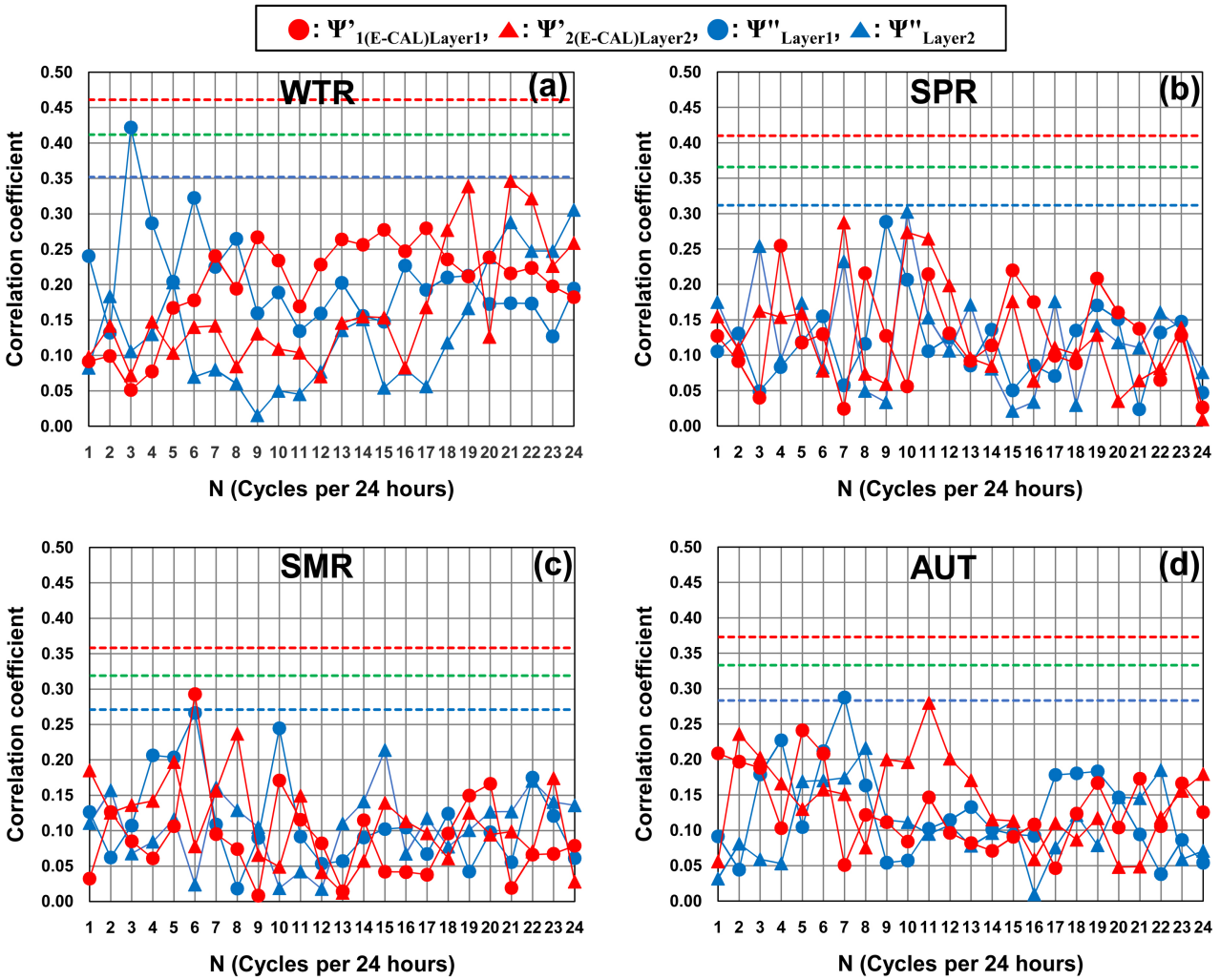

Figure 3. Correlation coefficients between the psi prime index $\Psi'_{1(E\text{-}CAL)Layer1}$, $\Psi'_{2(E\text{-}CAL)Layer2}$, psi double prime index Ψ''_{Layer1}, Ψ''_{Layer2} and their periodic approximation curves.

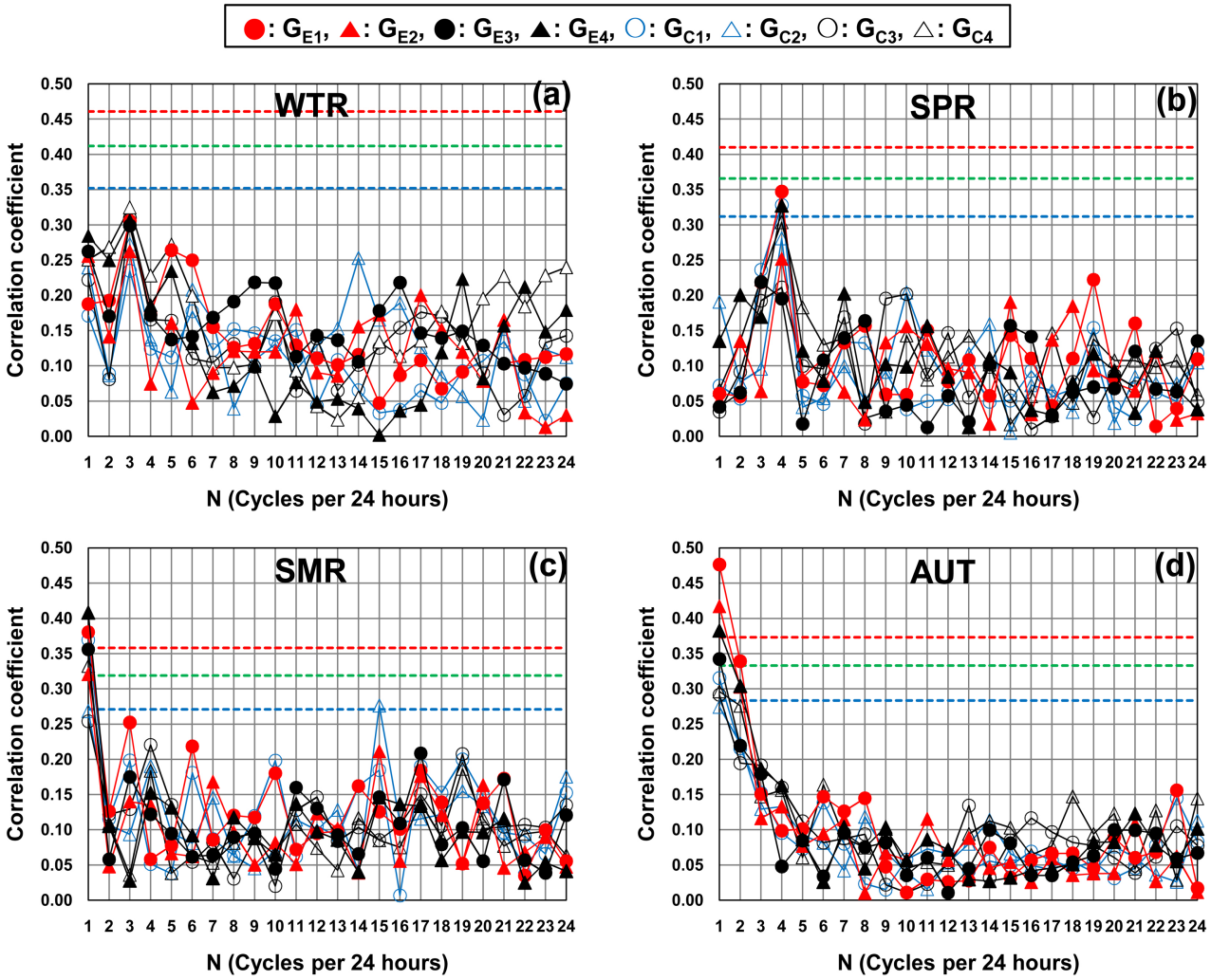

Figure 4. Correlation coefficients between the release gas concentrations (G_{E1}, G_{E2}, G_{E3}, G_{E4}, G_{C1}, G_{C2}, G_{C3}, G_{C4}) and their periodic approximations.

approximation curve per 24 hours, ranging from 1 to 24.

The three dashed lines in the figure represent the significance of correlation coefficients that vary depending on the number of data points. The red dashed line indicates $p = 10^{-5}$, the green dashed line indicates $p = 10^{-4}$ and the blue dashed line indicates $p = 10^{-3}$. Figures 4(a)-(d) correspond to WTR, SPR, SMR, and AUT, respectively.

Based on the results of Figure 4, we reported in a previous paper [33] that the one cycle of the circadian rhythm, periodic diurnal variation of the gas concentrations released from the biosensors is 8 hours (N = 3) for WTR, 6 hours (N = 4) for SPR, 24 hours (N = 1) for SMR and a mixture of 24 hours (N = 1) and 12 hours (N = 2) for AUT.

In fact, our conclusion that there is almost no periodic diurnal variation of the pyramid power and the Bio-Entanglement in the results of the analysis in Section 4 was partly based on the comparison of the correlation coefficient behavior in Figure 4 and Figure 3. That is, in Figures 4(a)-(d), the eight gas concentrations G_{E1}, G_{E2}, G_{E3}, G_{E4}, G_{C1}, G_{C2}, G_{C3} and G_{C4} uniformly peak at a particular N. On the other hand, in Figures 3(a)-(d), the psi indices $\Psi'_{1(E\text{-}CAL)Layer1}$, $\Psi'_{2(E\text{-}CAL)Layer2}$ and the psi prime indices Ψ''_{Layer1}, Ψ''_{Layer2} did not show a uniform peak at a particular N. However, there were three cases in Figure 3 where significant correlation was observed: 1) in Figure 3(a), with N = 3 in the Bio-Entanglement for the lower biosensor;

2) in Figure 3(c), with N = 6 in the pyramid power for the lower biosensor; and 3) in Figure 3(d), with N = 7 in the Bio-Entanglement for the lower biosensor. We cannot completely ignore the significance of these three data points, and we believe that it will be possible to determine in future experiments whether these results are meaningful as real phenomena or whether they have arisen due to insufficient data or experimental errors. As a result of this consideration, we concluded overall that the pyramid power and the Bio-Entanglement do not exhibit significant periodic diurnal oscillations.

Regarding the Bio-Entanglement, we would like to emphasize that it is not the result of plant communication [40-50], which has recently attracted attention. If the biosensors G_{E1} and G_{E2} at the PS apex were to transmit a warning to their surroundings using some kind of transmission medium that they had received the pyramid power, the effects would propagate almost equally to the other six biosensors, G_{E3}, G_{E4}, G_{C1}, G_{C2}, G_{C3}, and G_{C4}, and their reactions would be expected to be the same. The gas generation reactions of these six biosensors would be almost identical. However, the analysis results showed that a response was observed only for G_{C1} and G_{C2}, which are paired with G_{E1} and G_{E2} [27, 28]. From this, we believe that the phenomenon between G_{E1}, G_{E2} and their paired G_{C1}, G_{C2} is not simply a plant-to-plant communication, but rather an entangled state that persists even when they are disconnected, and we have named this phenomenon Bio-Entanglement.

6. CONCLUSION

In our previous report, we revealed that the volatile components (gas concentrations) released from the biosensors used to detect pyramid power, exhibit a periodic diurnal vibration. This led us to question whether pyramid power and Bio-Entanglement also have periodic diurnal oscillations, which we investigated. Based on the data, our conclusion is that pyramid power and Bio-Entanglement exhibit almost no periodic diurnal oscillation. Therefore, we speculate that the pyramid power near the PS apex is exerting a constant influence that we propose to be a type of static field. The pyramid power field is similar in that respect to an electric or magnetic field but possibly a novel type of static field worthy of further investigation. We expect that our research results will be widely accepted in the future and will become the foundation for a new research field in science, with a wide range of applications.

ACKNOWLEDGEMENTS

This research was funded by Science Peace Culture Foundation (SPC-F), (Chairman of the Board of Directors: Dr. Mikio Yamamoto).

CONFLICTS OF INTEREST

The authors declare no conflicts of interest regarding the publication of this paper.

REFERENCES

1. Ostrander, S. and Schroeder, L. (1970) Psychic Discoveries Behind the Iron Curtain. Prentice-Hall, Inc., Upper Saddle River.
2. Flanagan, P. (1973) Pyramid Power: The Science of the Cosmos. PhiSciences Press, Cottonwood.
3. Flanagan, P. (1973) Pyramid Power: The Millennium Science. Earthpulse Press, Inc., Anchorage.
4. Flanagan, P. (1981) Pyramid Power II: The Scientific Evidence. Innergy Publications, Tucson.
5. Toth, M. and Nielsen, G. (1974) Pyramid Power. Destiny Books, Rochester.
6. Schul, B. and Pettit, E. (1975) The Secret Power of Pyramids. Fawcett Gold Medal, New York.
7. Wyckoff, J. (1976) Using Pyramid Power. Kensington Publishing Corp., New York.
8. Stark, N. (1977) The First Practical Pyramid Book: Free Energy for Beauty, Health, Gardening, Food Dehydra-

tion, and Meditation. Sheed Andrews and McMeel, Inc., Kansas City.

9. King, S. (1977) Pyramid Energy Handbook. Warner Books, New York.
10. Gray, C.G. and Gray, V. (1979) Secrets from Beyond the Pyramids. The Alternative Universe Edmonton, Alberta.
11. Schul, B. and Pettit, E. (1979) Pyramid Power a New Reality. Stillpoint, Walpole.
12. Dunn, C. (1998) The Giza Power Plant: Technologies of Ancient Egypt. Bear & Company, Rochester.
13. Childress, D.H. (2000) Technology of the Gods: The Incredible Sciences of the Ancients. Adventures Unlimited Press, Kempton.
14. Elfouly, G. (2012) The Great Pyramid System: The Blue Light. An Amazon Company, North Charleston.
15. Creighton, S. and Osborn, G. (2012) The Giza Prophecy. Bear & Company, Rochester.
16. Kiss, Z.J. (2015) The Quantum Impulse and the Space-Time Matrix: The Power of the Hydrogen Process and the Pyramid. Trafford Publishing, Bloomington.
17. Lyke, S. (2018) The Great Pyramid's Laser Power Plant.
18. Brown, J.E., Hurtak, J.J. and Hurtak, D. (2019) Giza's Industrial Complex: Ancient Egypt's Electrical Power and Gas Generating Systems. Academy for Future Science, Los Gatos.
19. Rubik, B. (2016) Interactions of Pyramidal Structures with Energy and Consciousness. *The Journal of Natural and Social Philosophy*, **12**, 259-275. https://www.researchgate.net/publication/309407219
20. Takagi, O., Sakamoto, M., Kokubo, H., Yoichi, H., Kawano, K. and Yamamoto, M. (2013) Meditator's Non-Contact Effect on Cucumbers. *International Journal of Physical Sciences*, **8**, 647-651. https://doi.org/10.5897/IJPS2012.3800
21. Takagi, O., Sakamoto, M., Yoichi, H., Kokubo, H., Kawano, K. and Yamamoto, M. (2015) Discovery of an Anomalous Non-Contact Effect with a Pyramidal Structure. *International Journal of Sciences*, **4**, 42-51. https://doi.org/10.18483/ijSci.714
22. Takagi, O., Sakamoto, M., Yoichi, H., Kokubo, H., Kawano, K. and Yamamoto, M. (2016) An Unknown Force Awakened by a Pyramidal Structure. *International Journal of Sciences*, **5**, 45-56. https://doi.org/10.18483/ijSci.1038
23. Takagi, O., Sakamoto, M., Yoichi, H., Kokubo, H., Kawano, K. and Yamamoto, M. (2019) Discovery of an Un-Explained Long-Distance Effect Caused by the Association between a Pyramidal Structure and Human Unconsciousness. *Journal of International Society of Life Information Science*, **37**, 4-16. https://www.researchgate.net/publication/331917237
24. Takagi, O., Sakamoto, M., Yoichi, H., Kawano, K. and Yamamoto, M. (2019) Potential Power of the Pyramidal Structure. *Natural Science*, **11**, 257-266. https://doi.org/10.4236/ns.2019.118026
25. Takagi, O., Sakamoto, M., Yoichi, H., Kawano, K. and Yamamoto, M. (2020) Potential Power of the Pyramidal Structure II. *Natural Science*, **12**, 248-272. https://doi.org/10.4236/ns.2020.125022
26. Takagi, O., Sakamoto, M., Yoichi, H., Kawano, K. and Yamamoto, M. (2020) Potential Power of the Pyramidal Structure III: Discovery of Pyramid Effects with and without Seasonal Variation. *Natural Science*, **12**, 743-753. https://doi.org/10.4236/ns.2020.1212066
27. Takagi, O., Sakamoto, M., Kawano, K. and Yamamoto, M. (2021) Potential Power of the Pyramidal Structure IV: Discovery of Entanglement Due to Pyramid Effects. *Natural Science*, **13**, 258-272. https://doi.org/10.4236/ns.2021.137022
28. Takagi, O., Sakamoto, M., Kawano, K. and Yamamoto, M. (2021) Potential Power of the Pyramidal Structure V: Seasonal Changes in the Periodicity of Diurnal Variation of Biosensors Caused by Entanglement Due to Pyra-

mid Effects. *Natural Science*, **13**, 523-536. https://doi.org/10.4236/ns.2021.1312046

29. Takagi, O., Sakamoto, M., Kawano, K. and Yamamoto, M. (2022) Potential Power of the Pyramidal Structure VI: Pyramid Effects Due to Potential Power and Pyramid Effects Due to Bio-Entanglement. *Natural Science*, **14**, 251-263. https://doi.org/10.4236/ns.2022.146025
30. Takagi, O., Sakamoto, M., Kawano, K. and Yamamoto, M. (2023) Potential Power of the Pyramidal Structure VII: Effects of Pyramid Power and Bio-Entanglement on the Circadian Rhythm of Biosensors. *Natural Science*, **15**, 19-38. https://doi.org/10.4236/ns.2023.151003
31. Takagi, O., Sakamoto, M., Yoichi, H., Kokubo, H., Kawano, K. and Yamamoto, M. (2018) Discovery of Seasonal Dependence of Bio-Reaction Rhythm with Cucumbers. *International Journal of Science and Research Methodology*, **9**, 163-175. https://www.researchgate.net/publication/331917254
32. Takagi, O., Sakamoto, M., Yoichi, H., Kokubo, H., Kawano, K. and Yamamoto, M. (2018) Relationship between Gas Concentration Emitted from Cut Cucumber Cross Sections and Growth Axis. *International Journal of Science and Research Methodology*, **9**, 153-167. https://www.researchgate.net/publication/331917255
33. Takagi, O., Sakamoto, M., Kawano, K. and Yamamoto, M. (2022) Seasonal Changes in the Circadian Rhythm of Gas Released from Harvested Cucumbers. *Natural Science*, **14**, 503-516. https://doi.org/10.4236/ns.2022.1411045
34. Takagi, O., Sakamoto, M., Yoichi, H., Kokubo, H., Kawano, K. and Yamamoto, M. (2016) Necessary Condition of an Anomalous Phenomenon Discovered by a Pyramidal Structure. *Journal of International Society of Life Information Science*, **34**, 154-157. https://www.researchgate.net/publication/307283729
35. Takagi, O., Sakamoto, M., Yoichi, H., Kokubo, H., Kawano, K. and Yamamoto, M. (2019) Discovery from the Experiment on the Unexplained Functions of the Pyramidal Structure—The Phenomenon Caused by the Personal Relationship. *Journal of International Society of Life Information Science*, **37**, 60-65. https://www.researchgate.net/publication/331916903
36. Takagi, O., Sakamoto, M., Yoichi, H., Kawano, K. and Yamamoto, M. (2020) Scientific Elucidation of Pyramid Power: I. *Journal of International Society of Life Information Science*, **38**, 130-145. https://www.researchgate.net/publication/344603987
37. Takagi, O., Sakamoto, M., Yoichi, H., Kawano, K. and Yamamoto, M. (2020) Chapter 4. Meditator's Non-Contact Effect on Cucumbers. In: Rafatullah, M., Ed., *Theory and Applications of Physical Science*, Vol. 3, Book Publisher International, London, 105-113. https://www.researchgate.net/publication/339030704
38. Kokubo, H., Takagi, O. and Koyama, S. (2010) Application of a Gas Measurement Method-Measurement of Ki Fields and Non-Contact Healing. *Journal of International Society of Life Information Science*, **28**, 95-103. https://www.researchgate.net/publication/228957054
39. Kokubo, H., Koyama, S. and Takagi, O. (2010) Relationship between Biophotons and Gases Generated from Cucumber Pieces. *Journal of International Society of Life Information Science*, **28**, 84-94. https://www.researchgate.net/publication/267409897
40. Goodspeed, D., Liu, J.D., Chehab, E.W., Sheng, Z., Francisco, M., Kliebenstein, D.J. and Braam, J. (2013) Post-harvest Circadian Entrainment Enhances Crop Pest Resistance and Phytochemical Cycling. *Current Biology*, **23**, 1235-1241. https://doi.org/10.1016/j.cub.2013.05.034
41. McClung, C.R. (2011) The Genetics of Plant Clocks. In: *Advances in Genetics*, Vol. 74, Elsevier, Amsterdam, 105-139. https://doi.org/10.1016/B978-0-12-387690-4.00004-0
42. Endo, M., Shimizu, H., Nohales, M.A., Araki, T. and Kay, S.A. (2014) Tissue-Specific Clocks in Arabidopsis Show Asymmetric Coupling. *Nature*, **515**, 419-422. https://doi.org/10.1038/nature13919
43. Farmer, E.E. (2013) Surface-to-Air Signals. *Nature*, **411**, 854-856. https://doi.org/10.1038/35081189

44. Ozawa, R., Arimura, G., Takabayashi, J., Shimoda, T. and Nishioka, T. (2000) Involvement of Jasmonate- and Salicylate-Related Signaling Pathways for the Production of Specific Herbivore-Induced Volatiles in Plants. *Plant and Cell Physiology*, **41**, 391-398. https://doi.org/10.1093/pcp/41.4.391

45. De Moraes, C.M., Mescher, M.C. and Tumlinson, J.H. (2001) Caterpillar-Induced Nocturnal Plant Volatiles Repel Conspecific Females. *Nature*, **410**, 577-580. https://doi.org/10.1038/35069058

46. Yoneya, K. and Takabayashi, J. (2014) Plant-Plant Communication Mediated by Airborne Signals: Ecological and Plant Physiological Perspectives. *Plant Biotechnology*, **31**, 409-416. https://doi.org/10.5511/plantbiotechnology.14.0827a

47. Šimpraga, M., Takabayashi, J. and Holopainen, J.K. (2016) Language of Plants: Where Is the Word? *Journal of Integrative Plant Biology*, **58**, 343-349. https://doi.org/10.1111/jipb.12447

48. Pélissier, R., Violle, C. and Morel, J.B. (2021) Plant Immunity: Good Fences Make Good Neighbors? *Current Opinion in Plant Biology*, **62**, Article ID: 102045. https://doi.org/10.1016/j.pbi.2021.102045

49. Marmolejo, L.O., Thompson, M.N. and Helms, A.M. (2021) Defense Suppression through Interplant Communication Depends on the Attacking Herbivore Species. *Journal of Chemical Ecology*, **47**, 1049-1061. https://doi.org/10.1007/s10886-021-01314-6

50. Suda, H. and Toyota, M. (2022) Integration of Long-Range Signals in Plants: A Model for Wound-Induced Ca^{2+}, Electrical, ROS, and Glutamate Waves. *Current Opinion in Plant Biology*, **69**, Article ID: 102270. https://doi.org/10.1016/j.pbi.2022.102270